Bol. Soc. Paran. Mat.
©SPM – E-ISSN-2175-1188
SPM: www.spm.uem.br/bspm

(3s.) **v. 2026 (44)** : 1–28.
ISSN-0037-8712
doi:10.5269/bspm.79514

The Impact of Vaccination on a Nonlinear Ebola Virus Disease Mathematical Model

Nnaemeka Stanley Aguegboh, Chukwudi Okoye, Chinedu Kingsley Friday and Chioma Lydia Ejikeme

ABSTRACT: This study examines the spread of Ebola Virus Disease (EVD) among human populations by creating a nonlinear mathematical model that assesses the effects of vaccination. The analysis shows that the equilibrium without disease (DFE) maintains local stability when the associated reproduction number ($\mathcal{R}_0$) is below one. Conversely, the DFE loses global stability, whereas the endemic equilibrium (EE) achieves global stability. The presence of the endemic equilibrium is established for all values where $\mathcal{R}_0 > 1$. Sensitivity analysis reveals that the infection rate (β_2) among susceptible individuals has a dominant effect on $\mathcal{R}_0$, emphasizing the critical need for interventions targeting susceptible populations. Furthermore, vaccination (τ) significantly influences the epidemic management, as lower vaccination rate lead to persistently elevated $\mathcal{R}_0$ values. The findings underscore the importance of high vaccination coverage to mitigate disease transmission. Numerical simulations, performed using MATLAB, compare the model's predictions with analytical results and highlight the global impact of vaccination and public response on disease control.

Keywords: Ebola, vaccination, non-linear model, impact.

Contents

1. Introduction

Ebola is a severe illness attributed to the Ebola virus which belongs to the Filoviridae family [1]. This disease impacts humans as well as various non-human primates, including monkeys, fruit bats, chimpanzees, antelopes, gorillas, and porcupines, which are often discovered ill or deceased within rainforest regions [2,3]. Since its first emergence in Sudan and the Democratic Republic of Congo (DRC) in 1976, there have been over 20 outbreaks recorded across central and eastern Africa [4,5]. Notably, no cases were reported between 1979 and 1994; however, outbreaks have occurred with increasing regularity since then [6,7]. Between August 2013 and June 2016, West Africa witnessed its most extensive outbreak, heavily impacting Sierra Leone, Liberia, and Guinea. Over 28,000 cases were recorded during this time,

2020 *Mathematics Subject Classification:* 92D30, 34D23.
Submitted October 13, 2025. Published June 05, 2026.

resulting in roughly 11,000 fatalities, as urban areas saw swift disease transmission [8,9]. The outbreak also led to the detection of imported cases in the US, Spain, Italy, the UK, Senegal, Mali, and Nigeria [10,11]. By February 11, 2015, the cumulative cases had reached 22,859, with 9,162 recorded deaths [12].

The Ebola virus consists of six known species, four of which Ebola Ivory Coast (currently known as Tai Forest Virus, TAFV), Sudan Ebola Virus (SUDV), Zaire Ebola Virus (EBOV), and Bundibugyo Ebola Virus (BDBV) are responsible for human infections [13]. The other two species, Bombali and Reston (RESTV), predominantly infect non-human primates [14]. RESTV identified in 1989 within a monkey colony imported from the Philippines to Reston, Virginia, USA [15]. Since then, it has been linked to outbreaks in locations such as Philadelphia, Pennsylvania, Alice, Texas, and Sienna, Italy. Bombali Ebola Virus, discovered in Sierra Leone in 2018 in bats, has not yet been shown to cause disease in humans [16,4,1,17]. Although Ebola Virus Disease is believed to originate from animals, the exact natural reservoir remains unidentified despite extensive studies [18]. Non-human primates, while capable of transmitting the virus to humans, are unlikely to serve as reservoirs because they develop severe and often fatal illnesses upon infection [19]. Before the outbreaks started in DRC and Gabon, numerous animal carcasses were discovered in the impacted areas, and testing revealed infections from various sources [13].

The first recorded human case of EVD was linked to direct contact with the blood, organs, bodily fluids, or secretions of infected animals such as bats, in addition to exposure to contaminated needles or clothing [6]. Ebola Virus Disease (EVD) has been documented in people who came into contact with infected wildlife, such as gorillas, chimpanzees, and forest antelopes whether alive or dead in areas like the Republic of Congo, Côte d'Ivoire, and Gabon [26]. Additionally, outbreaks have been linked to traditional burial rituals that involve mourners physically handling the bodies of the deceased [20,21]. Sexual transmission has also been reported in some recovered patients, with evidence demonstrating that the virus can linger within semen for months after recovery [12]. The incubation period for EVD spans from 2 to 21 days, while the contagious phase generally lasts between 4 and 10 days [22]. Symptoms typically appear abruptly and are characterized by headaches, fever, muscle cramps, joint pains, extreme exhaustion, and a sore throat [23]. These are often followed by vomiting, diarrhea, rashes, and signs of kidney or liver impairment, along with internal and external bleeding [24]. Laboratory findings commonly indicate a decrease in leukocyte and platelet concentration, alongside liver enzyme activity increase. The case fatality rate of EVD varies between 25% and 90%, depending on factors like the specific virus strain and the age of the patient, immune system effectiveness, and other relevant conditions [25,23].

The Food and Drug Administration (FDA) of the United States, on December 19, 2019, granted approval to rVSV-ZEBOV, commercially known as Ervebo, making it the first officially licensed vaccine against Ebola Virus [26,27]. Ervebo has demonstrated both safety and efficacy for safeguarding against the Zaire Ebola Virus species. The Strategic Advisory Group of Experts (SAGE) on Immunization endorses the use of this vaccine as an essential component of a broader strategy for managing Ebola outbreaks [25]. Following the "expanded access and compassionate use" guidelines, about 16,000 people in 2015 received Ervebo in Guinea and approximately 300,000 received it between 2018 and 2020 in DRC [28,25]. While it is officially approved for individuals aged 18 and above, excluding lactating and pregnant women [29], the application of the vaccine was broadened throughout the 2018–2020 epidemic in DRC across South Kivu, Ituri, and North Kivu. Under compassionate use protocols and following SAGE recommendations, it was also administered to children above six months, as well as to lactating and pregnant women [31,26,30]. Clinical trials demonstrated that the vaccine provided 100% protection against Ebola Virus Disease beginning ten days post administration [32]. While the exact duration of immunity is still unclear, the single-dose effectiveness of the vaccine stands out, as most vaccines require multiple doses to provide full protection [33]. However, it is crucial to emphasize that Ervebo has not been evaluated in individuals with weakened immune systems or those on immunosuppressive therapies [34,35]. As a result, the vaccine's effectiveness in these groups remains unknown, and such individuals may face increased risks from live attenuated vaccines [36].

The European Medicines Agency recommended in May 2020 the approval of a second Ebola vaccine regimen for individuals aged one year and older. This regimen, comprising two doses Mvabea (MVA-BN-Filo) and Zabdeno (Ad26.ZEBOV) was proposed for use in the fight against Ebola [26,18]. In this regimen, Zabdeno is administered as the initial dose, followed by Mvabea approximately eight weeks later

as a second dose [37,38]. However, this two-dose prophylactic regimen is unsuitable for outbreak responses requiring immediate protection [39]. A booster dose of Zabdeno is advised for healthcare officials four months following the second dose [26]. The efficacy of Zabdeno and Mvabea were evaluated in several clinical studies involving thousands of participants, including children, adolescents, and adults, conducted across the United States, Africa, and Europe [39,32]. These research demonstrated that vaccination protocol is both safe and effective in triggering an immune defense against the EVD [25,9]. Recovery from EVD depends on effective supportive care and the strength of the patient's immune system. It remains unclear whether individuals who recover from EVD acquire lifelong immunity or are susceptible to reinfection with a different Ebola virus species [40]. Some survivors may experience long-term health complications, such as joint and vision issues, memory loss, neck swelling, and dry mouth [41].

The significant public health burden imposed by Ebola Virus Disease (EVD) has motivated the application of mathematical modeling to better understand its transmission dynamics and identify effective control strategies [42,10]. [43] analyzed the exposed-to-susceptible (E/S) ratio within a SEIR disease model during the outbreak of 2014–2016, demonstrating that its maximum value occurs when the reproduction number (R_t) approaches one. They also introduced the Cross Point (CP) as a critical metric for epidemic monitoring. [13] constructed an SEIR model to explore Ebola virus dynamics, performing stability computations for the no disease and endemic state and proving global stability using Lyapunov functions. Their study revealed that a non-standard finite difference (NSFD) scheme outperforms the Runge–Kutta (RK4) method in preserving the model's dynamics. [44] investigated EVD spread in Liberia, calculating $R_0 = 2.012$ and emphasizing the significant role of transmission coefficients. Their findings showed that combining preventive strategies, including quarantine protocols and secure burial practices can reduce R_0 below one, thereby containing the outbreak effectively. [45] presents a model of EVD, incorporating safe burial practices and environmental contamination. The model shows forward bifurcation, suggesting that reducing R_0 can control Ebola spread. Numerical simulations without optimal control highlight strategies like reducing interactions with infected individuals, public education, vaccination, and secure burial as effective control measures. [46] created a model to evaluate how various interventions affect Ebola transmission. They estimated the basic reproduction numbers as 1.2552 for Guinea, 1.6093 for Sierra Leone, and 1.7994 for Liberia. They emphasized that enhancing isolation effectiveness, minimizing burial delays, and leveraging media coverage are vital for controlling the epidemic and reducing its size. [47] investigated an Ebola epidemic model that incorporates density-dependent treatment and a nonlinear incidence rate. Their findings highlighted the potential for backward bifurcation and bi-stability under specific conditions. The study emphasizes the importance of swift behavioral changes and effective treatment strategies for controlling outbreaks, with numerical validation using data from the Kivu outbreak that occurred between 2018 and 2020.

The current research focuses on the development of an autonomous deterministic model to explore how EVD spreads. This is designed to assess the effect of vaccination on individuals infected with the virus. Additionally, the goal of this research is to investigate the influence of public enlightenment on abating the transmission of the virus across various demographic groups, including the susceptible, infected, infectious, and quarantined-infectious populations.

2. Title Material

In this study, the system's dynamics are modeled mathematically using an autonomous system of differential equations. This approach is utilized to guarantee the study's effectiveness and to offer a deeper understanding of the research analysis. The compartmental equations were analyzed using various mathematical tools. These include positivity and boundedness analysis, classification of fixed (equilibrium) points, Jacobian transformation for stability analysis, and numerical simulations performed using MATLAB.

2.1. Model Formulation and Analysis

The model is compartmental, dividing the population into various classes based on their disease status. Table 1 presents the descriptions of the model's state variables and parameters.

Table 1: State Variables and Parameters for the Ebola Virus Model (with units)

Variable/Parameter	Description	Value	Unit	Reference
State Variables				
S_v	Susceptible vaccinated human population	$5,000$	persons	Estimated
S	Susceptible human population	$3,441,790$	persons	[44]
I_1	Latently infected humans of category one	20	persons	[44]
I_2	Latently infected humans of category two	29	persons	[44]
Q	Quarantined humans	20	persons	[44]
R	Recovered humans	23	persons	[44]
Model Parameters				
β_1	Infection rate for vaccinated individuals	0.2896	person^{-1} day^{-1}	[46]
β_2	Infection rate for susceptible individuals	0.275	person^{-1} day^{-1}	[46]
α_1	Rate of transition from I_1 to I_2	0.8333	day^{-1}	Estimated
α_2	Rate of transition from I_2 to Q	0.07143	day^{-1}	[21]
δ_1	Ebola-induced death rate in infectious individuals	0.11386	day^{-1}	[21]
ϕ	Rate at which vaccinated become susceptible	0.062	day^{-1}	Estimated
δ_2	Ebola-induced death rate in Q	0.0901	day^{-1}	[44]
γ_1	Recovery rate of latently infected individuals (category one)	0.167	day^{-1}	[46]
μ	Natural death rate	0.0067	day^{-1}	[13]
γ_2	Recovery rate of Q	0.17	day^{-1}	[21]
Λ	Recruitment rate	0.3321	persons day^{-1}	[48]
τ	Vaccination rate of susceptible individuals	0.5	day^{-1}	Estimated
p	Fraction of vaccinated individuals	0.5	dimensionless	Estimated

The following assumptions form the basis of the model:

1. Vaccination is for the entire population (mass action incidence).

2. There is a homogeneous mixing (men and women alike).

3. There is Herd Immunity (An individual that recovers from the Ebola Virus infection does not become prone to the disease again).

4. The infected individuals will be of two categories namely:

   (a) Latently infected individuals of category one;

   (b) Latently infected individuals of category two.

   Where category one represents the incubation period with mild symptoms between 2-7 days. At this point, the individuals could not transmit the Ebola Virus, while category two shows severe symptoms. At this point, the individuals are infectious and have the capacity to infect others.

5. Public enlightenment is used as the control measure denoted by p, and only a fraction $(1-p)$ of those that accept enlightenment takes the vaccine.

6. Latently infected individuals of category two move to isolation centres or get quarantined.

7. The latently infected individuals of category one will also recover.

Figure 1 below shows the model's flow diagram:

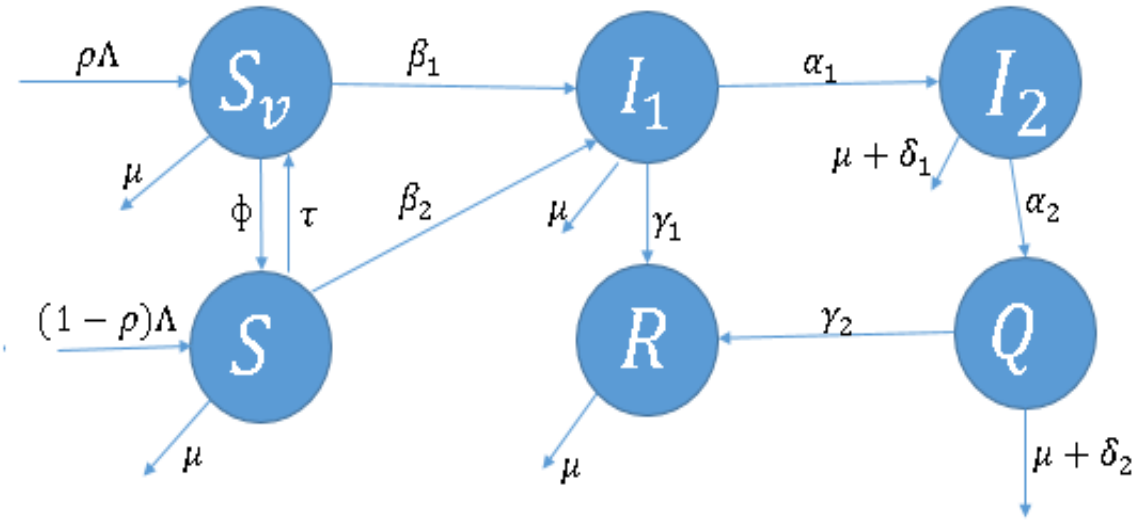

Figure 1: Evolution of the population over time.

The evolving behavior of the system is described by the model:

$$\frac{dS_v}{dt} = p\Lambda + \tau S - \beta_1 S_v I_2 - \phi S_v - \mu S_v, \tag{2.1}$$

$$\frac{dS}{dt} = (1-p)\Lambda + \phi S_v - \tau S - \beta_2 S I_2 - \mu S, \tag{2.2}$$

$$\frac{dI_1}{dt} = (\beta_1 S_v + \beta_2 S) I_2 - (\alpha_1 + \gamma_1 + \mu) I_1, \tag{2.3}$$

$$\frac{dI_2}{dt} = \alpha_1 I_1 - (\alpha_2 + \delta_1 + \mu) I_2, \tag{2.4}$$

$$\frac{dQ}{dt} = \alpha_2 I_2 - (\delta_2 + \gamma_2 + \mu) Q, \tag{2.5}$$

$$\frac{dR}{dt} = \gamma_2 Q + \gamma_1 I_1 - \mu R. \tag{2.6}$$

The model equations account for the recruitment of susceptible individuals, vaccination, exposure to the virus, progression of the disease, quarantine, recovery, and Ebola-induced mortality. The relationships between these compartments illustrate the process by which the disease disseminates throughout the entire population. Through the analysis of this system, we seek to evaluate the impact of different public health measures and control strategies.

2.2. Invariant Region

The invariant region is defined as the set of values where the model's solutions persist and is biologically meaningful. To ensure this condition, we assume that the parameters and variables are always non-negative when $t \geq 0$.

Define the region Ω as:

$$\Omega = \left\{ (S_v, S, I_1, I_2, Q, R) \in \mathbb{R}^6_+ : N(t) \leq \frac{\Lambda}{\mu} \right\},$$

$N(t) = S_v(t) + S(t) + I_1(t) + I_2(t) + Q(t) + R(t).$

Lemma 2.1 *The solution set*

$$(S_v, S, I_1, I_2, Q, R) \in \mathbb{R}^6_+$$

remains positive for $t > 0$ *if*

$$(S_v^0, S^0, I_1^0, I_2^0, Q^0, R^0) \geq 0 \in \Omega.$$

Proof: By definition, the initial conditions

$$(S_v^0, S^0, I_1^0, I_2^0, Q^0, R^0) \geq 0$$

ensure non-negativity for $t > 0$. We now show that these initial conditions are contained within the region Ω.

Consider the rate of variation of the population:

$$\frac{dN}{dt} = \frac{dS_v}{dt} + \frac{dS}{dt} + \frac{dI_1}{dt} + \frac{dI_2}{dt} + \frac{dQ}{dt} + \frac{dR}{dt}.$$

Simplifying the terms, we get:

$$\begin{aligned} \frac{dN}{dt} &= \Lambda - \mu N - \delta_1 I_2 - \delta_2 Q \\ &< \Lambda - \mu N. \end{aligned}$$

This represents a linear differential equation of the first order, and its solution can be found in [49]:

$$N(t) \leq \frac{\Lambda}{\mu} + \left(N(0) - \frac{\Lambda}{\mu}\right) e^{-\mu t}.$$

$e^{-\mu t} \to 0$ as $t \to \infty$.
Therefore, $N(t) \to \frac{\Lambda}{\mu}$. □

This proof ensures that the model is both mathematically sound and epidemiologically relevant. By confirming that the population remains non-negative and bounded within the region Ω, we guarantee that the model's solutions are biologically valid for all future times $t \geq 0$.

2.3. Equilibrium State Without Disease (DFE)

Disease-free equilibrium represents a state where EVD is entirely absent. At Disease-free equilibrium, the compartments for infected individuals (I_1 and I_2), quarantined individuals (Q), and recovered individuals (R) are all zero. The Disease-free equilibrium can be expressed as:

$$E^0 = (S_v^0, S^0, I_1^0, I_2^0, Q^0, R^0),$$

where:

$$\begin{aligned} I_1^0 &= 0, \\ I_2^0 &= 0, \\ Q^0 &= 0, \\ R^0 &= 0. \end{aligned}$$

To determine the equilibrium values for the susceptible vaccinated (S_v) and susceptible (S) compartments, we solve the following equations:

From Equation 2.2:

$$p\Lambda + \tau S = (\phi + \mu) S_v. \tag{2.7}$$

From Equation 2.3:

$$(1-p)\Lambda + \phi S_v = \tau S + \mu S. \tag{2.8}$$

Substituting Equation 2.7 into Equation 2.8:

$$(1-p)\Lambda + \phi\left(\frac{p\Lambda + \tau S}{\phi + \mu}\right) = \tau S + \mu S.$$

This simplifies to:

$$S_v = \frac{\Lambda(\mu p + \tau)}{\mu(\mu + \phi + \tau)}, \quad S = \frac{\Lambda(\mu - \mu p + \phi)}{\mu(\mu + \phi + \tau)}$$

Thus,

$$E^0 = \left(\frac{\Lambda(\mu p + \tau)}{\mu(\mu + \phi + \tau)}, \frac{\Lambda(\mu - \mu p + \phi)}{\mu(\mu + \phi + \tau)}, 0, 0, 0, 0\right).$$

2.4. Fundamental Reproduction Metric $\mathcal{R}_0$ of the Model

We compute the basic reproduction number R_0 using the next generation matrix method [50,51] The infected compartments of system (2.1)–(2.6) are

$$x = (I_1, I_2, Q)^T.$$

However, only I_1 and I_2 contribute directly to the generation of new infections. The quarantined class Q does not produce new infections. From the model equations, the rate of new infections entering I_1 is

$$\mathcal{F}_1 = (\beta_1 S_v + \beta_2 S) I_2,$$

while no new infections enter I_2 or Q. Thus,

$$\mathcal{F} = \begin{pmatrix} (\beta_1 S_v + \beta_2 S) I_2 \\ 0 \\ 0 \end{pmatrix}.$$

The remaining transfer terms are

$$\mathcal{V} = \begin{pmatrix} (\alpha_1 + \gamma_1 + \mu) I_1 \\ (\alpha_2 + \delta_1 + \mu) I_2 - \alpha_1 I_1 \\ (\delta_2 + \gamma_2 + \mu) Q - \alpha_2 I_2 \end{pmatrix}.$$

At the disease-free equilibrium

$$E^0 = (S_v^0, S^0, 0, 0, 0, 0),$$

where

$$S_v^0 = \frac{p\Lambda}{\mu + \phi}, \qquad S^0 = \frac{(1-p)\Lambda}{\mu}.$$

Linearizing around E^0, we compute the Jacobian matrices

$$F = D\mathcal{F}(E^0), \qquad V = D\mathcal{V}(E^0).$$

Thus,

$$F = \begin{pmatrix} 0 & \beta_1 S_v^0 + \beta_2 S^0 & 0 \\ 0 & 0 & 0 \\ 0 & 0 & 0 \end{pmatrix},$$

and

$$V = \begin{pmatrix} \alpha_1 + \gamma_1 + \mu & 0 & 0 \\ -\alpha_1 & \alpha_2 + \delta_1 + \mu & 0 \\ 0 & -\alpha_2 & \delta_2 + \gamma_2 + \mu \end{pmatrix}.$$

The next generation matrix is

$$K = FV^{-1}.$$

Since Q does not contribute to new infections, the spectral radius reduces to the dominant term involving I_1 and I_2.

After computation, we obtain

$$R_0 = \frac{(\beta_1 S_v^0 + \beta_2 S^0)\alpha_1}{(\alpha_1 + \gamma_1 + \mu)(\alpha_2 + \delta_1 + \mu)}.$$

Final expression. Substituting S_v^0 and S^0, we have

$$R_0 = \frac{\alpha_1 \left(\beta_1 \dfrac{p\Lambda}{\mu + \phi} + \beta_2 \dfrac{(1-p)\Lambda}{\mu} \right)}{(\alpha_1 + \gamma_1 + \mu)(\alpha_2 + \delta_1 + \mu)}.$$

This completes the proof.

2.5. The Endemic Equilibrium (EE)

At EE, the compartments I_1, I_2, Q, and R attain non-zero values. From equation **??**, we have

$$\frac{dR^*}{dt} = \gamma_2 Q^* + \gamma_1 I_1 - \mu R^* = 0 \tag{2.9}$$

$$R^* = \frac{\gamma_2 Q^* + \gamma_1 I_1^*}{\mu} \tag{2.10}$$

From equation 2.6,

$$\frac{dQ^*}{dt} = \alpha_2 I_2^* - (\delta_2 + \gamma_2 + \mu)Q^* = 0 \tag{2.11}$$

$$Q^* = \frac{\alpha_2 I_2^*}{(\delta_2 + \gamma_2 + \mu)} \tag{2.12}$$

$$\frac{dI_2^*}{dt} = \alpha_1 I_1^* - (\alpha_2 + \delta_1 + \mu)I_2^* = 0 \tag{2.13}$$

$$I_2^* = \frac{\alpha_1 I_1^*}{(\alpha_2 + \delta_1 + \mu)} \tag{2.14}$$

Substituting equation 2.14 into equation 2.12, we have

$$Q^* = \frac{\alpha_1 \alpha_2 I_1^*}{(\alpha_2 + \delta_1 + \mu)(\delta_2 + \gamma_2 + \mu)} \tag{2.15}$$

Substituting equation 2.15 into equation 2.10, we have

$$R^* = \left[\frac{\gamma_2 \alpha_1 \alpha_2}{\mu(\alpha_2 + \delta_1 + \mu)(\delta_2 + \gamma_2 + \mu)} + \frac{\gamma_1}{\mu} \right] I_1^* \tag{2.16}$$

From equation 2.4, we have

$$\frac{dI_1^*}{dt} = (\beta_1 S_v^* + \beta_2 S^*) I_1^* - (\alpha_1 + \gamma_1 + \mu) I_1^* = 0$$

$$((\beta_1 S_v^* + \beta_2 S^*) - (\alpha_1 + \gamma_1 + \mu)) I_1^* = 0$$

Since $I_1^* \neq 0$, then

$$\beta_1 S_v^* + \beta_2 S^* = (\alpha_1 + \gamma_1 + \mu)$$

Hence, we have

$$S^* = \frac{(\alpha_1 + \gamma_1 + \mu) - \beta_1 S_v^*}{\beta_2} \tag{2.17}$$

and

$$S_v^* = \frac{(\alpha_1 + \gamma_1 + \mu) - \beta_1 S^*}{\beta_1} \tag{2.18}$$

From equation 2.3, we have

$$\frac{dS^*}{dt} = (1-p)\Lambda + \phi S_v^* - \tau S^* - \beta_2 S^* I_1^* - \mu S^* = 0$$

$$S^* = \frac{(1-p)\Lambda + \phi S_v^*}{\beta_2 I_1^* + \tau + \mu} \tag{2.19}$$

Substituting 2.19 into equ. 2.17, we have

$$S_v^* = \frac{\beta_2((\alpha_1 + \gamma_1 + \mu)(\beta_1 I_1^* + \tau + \mu) - \Lambda\beta_1 p)}{\beta_1[\beta_1\tau + \beta_2(\beta_1 I_1^* + \tau + \mu)]} - \frac{(\alpha_1 + \gamma_1 + \mu)}{\beta_1} \tag{2.20}$$

Substituting 2.20 into equ. 2.18, we have

$$S^* = \frac{(\alpha_1 + \gamma_1 + \mu)(\beta_1 I_1^* + \tau + \mu) - \Lambda\beta_1 p}{\beta_1\tau + \beta_2(\beta_1 I_1^* + \tau + \mu)} \tag{2.21}$$

$$\begin{aligned}
S_v^* &= \frac{\beta_2((\alpha_1 + \gamma_1 + \mu)(\beta_1 I_1^* + \tau + \mu) - \Lambda\beta_1 p)}{\beta_1[\beta_1\tau + \beta_2(\beta_1 I_1^* + \tau + \mu)]} - \frac{(\alpha_1 + \gamma_1 + \mu)}{\beta_1}, \\
S^* &= \frac{(\alpha_1 + \gamma_1 + \mu)(\beta_1 I_1^* + \tau + \mu) - \Lambda\beta_1 p}{\beta_1\tau + \beta_2(\beta_1 I_1^* + \tau + \mu)}, \\
I_1^* &= I_1^*, \\
I_2^* &= \frac{\alpha_1 I_1^*}{(\alpha_2 + \delta_1 + \mu)}, \\
Q^* &= \frac{\alpha_1\alpha_2 I_1^*}{(\alpha_2 + \delta_1 + \mu)(\delta_2 + \gamma_2 + \mu)}, \\
R^* &= \left[\frac{\gamma_2\alpha_1\alpha_2}{\mu(\alpha_2 + \delta_1 + \mu)(\delta_2 + \gamma_2 + \mu)} + \frac{\gamma_1}{\mu}\right] I_1^*.
\end{aligned}$$

Therefore, the endemic equilibrium point is:

$$E^* = (S_v^*, S^*, I_1^*, I_2^*, Q^*, R^*).$$

2.6. Stability Analysis

Stability analysis is crucial for understanding the persistence or eradication of infectious diseases within populations. By examining the stability of equilibrium states, we can determine the conditions under which disease outbreaks may occur, stabilize, or decline. Moreover, stability analysis allows us to assess the effect of control measures on the transmission of diseases, highlighting the impact of vaccination programs and public health measures [52].

2.6.1. Local Stability of the Equilibrium with No Disease.

Definition 2.1 *Consider the dynamical system defined by equations (2.1)–(2.6). An equilibrium point x achieves stability if all eigenvalues of the Jacobian matrix J, computed at x, possess strictly negative real parts. Conversely, instability arises at x when at least one eigenvalue of J exhibits a positive real part [53].*

Theorem 2.1 *The equilibrium point where no disease is present is locally unstable when $\mathcal{R}_0 > 1$ and stable when $\mathcal{R}_0 < 1$ [54].*

Proof: The Jacobian evaluated at DFE is:

$$J(E^0) = \begin{pmatrix} -(\phi+\mu) & \tau & -\beta_1 S_v^0 & 0 & 0 & 0 \\ \phi & -(\tau+\mu) & -\beta_2 S^0 & 0 & 0 & 0 \\ 0 & 0 & \beta_1 S_v^0 + \beta_2 S^0 - (\alpha_1+\gamma_1+\mu) & 0 & 0 & 0 \\ 0 & 0 & \alpha_1 & -(\alpha_2+\delta_1+\mu) & 0 & 0 \\ 0 & 0 & 0 & \alpha_2 & -(\delta_2+\gamma_2+\mu) & 0 \\ 0 & 0 & \gamma_1 & 0 & \gamma_2 & -\mu \end{pmatrix}$$

$$J(E^0) = \begin{pmatrix} -(\phi+\mu) & \tau & -\beta_1 S_v^0 & 0 & 0 & 0 \\ \phi & -(\tau+\mu) & -\beta_2 S^0 & 0 & 0 & 0 \\ 0 & 0 & (\alpha_1+\gamma_1+\mu)[\mathcal{R}_0 - 1] & 0 & 0 & 0 \\ 0 & 0 & \alpha_1 & -(\alpha_2+\delta_1+\mu) & 0 & 0 \\ 0 & 0 & 0 & \alpha_2 & -(\delta_2+\gamma_2+\mu) & 0 \\ 0 & 0 & \gamma_1 & 0 & \gamma_2 & -\mu \end{pmatrix}$$

Thus,

$$\mathrm{Tr}(J(E^0)) = -(\phi+\tau+2\mu) + (\alpha_1+\gamma_1+\mu)[\mathcal{R}_0 - 1] - (\alpha_2+\delta_1+\mu) - (\delta_2+\gamma_2+\mu) - \mu$$

Now, let

$$J(E^0) = \begin{pmatrix} -m_1 & m_2 & -m_3 & 0 & 0 & 0 \\ m_4 & -m_5 & -m_6 & 0 & 0 & 0 \\ 0 & 0 & m_7 & 0 & 0 & 0 \\ 0 & 0 & m_8 & -m_9 & 0 & 0 \\ 0 & 0 & 0 & m_{10} & -m_{11} & 0 \\ 0 & 0 & m_{12} & 0 & m_{13} & -m_{14} \end{pmatrix}$$

Correspondence of m_i with the original entries:

$$\begin{aligned} m_1 &= \phi + \mu, & m_2 &= \tau, & m_3 &= \beta_1 S_v^0, \\ m_4 &= \phi, & m_5 &= \tau + \mu, & m_6 &= \beta_2 S^0, \\ m_7 &= (\alpha_1+\gamma_1+\mu)(\mathcal{R}_0 - 1), & m_8 &= \alpha_1, & m_9 &= \alpha_2 + \delta_1 + \mu, \\ m_{10} &= \alpha_2, & m_{11} &= \delta_2 + \gamma_2 + \mu, & m_{12} &= \gamma_1, \\ m_{13} &= \gamma_2, & m_{14} &= \mu. \end{aligned}$$

Using Python symbolic computation, Determinant of J is obtained as:

$$\text{Det}(J) = -m_{11} \cdot m_{14} \cdot m_7 \cdot m_9 \cdot (m_1 \cdot m_5 - m_2 \cdot m_4)$$

Substituting the values of m_i, we have

$$\text{Det}(J) = -(\delta_2 + \gamma_2 + \mu) \cdot \mu^2 \cdot (\alpha_1 + \gamma_1 + \mu)(\mathcal{R}_0 - 1) \cdot (\alpha_2 + \delta_1 + \mu) \cdot (\tau + \phi + \mu)$$

Upon examining J at DFE, we find that for $\mathcal{R}_0 < 1$, the trace of the Jacobian matrix, $\text{Tr}(J)$, takes a negative value, while its determinant, $\text{Det}(J)$, remains positive. The negative trace of the Jacobian indicates the presence of a net inward flow of the system, while the positive determinant suggests that the equilibrium is stable in at least one direction. The stability of DFE is determined by $\mathcal{R}_0 < 1$, implying that if the model reproduction number falls below unity, the disease will ultimately be eradicated. Consequently, the system will revert to the disease-free state over time. This highlights the critical role of $\mathcal{R}_0$ in determining the DFE's stability. Specifically, when $\mathcal{R}_0$ is below one, the system remains in a stable, disease-free condition, supporting the conclusion that reducing $\mathcal{R}_0$ to values less than unity through effective control strategies will result in the eradication of the disease [55]. □

2.6.2. Local Stability of EE.

Theorem 2.2 *The EE is stable if $\mathcal{R}_0 > 1$, whereas it becomes unstable when $\mathcal{R}_0 < 1$ [56].*

Proof: The Jacobian of the system (2.1)-(2.6) is given as:

$$J = \begin{pmatrix} -\beta_1 I_1^* - \phi - \mu & \tau & -\beta_1 S_v^* & 0 & 0 & 0 \\ \phi & -\beta_2 I_1^* - \tau - \mu & -\beta_2 S^* & 0 & 0 & 0 \\ \beta_1 I_1^* & \beta_2 I_1^* & \beta_1 S_v^* + \beta_2 S^* - (\alpha_1 + \gamma_1 + \mu) & 0 & 0 & 0 \\ 0 & 0 & \alpha_1 & -(\alpha_2 + \delta_1 + \mu) & 0 & 0 \\ 0 & 0 & 0 & \alpha_2 & -(\delta_2 + \gamma_2 + \mu) & 0 \\ 0 & 0 & \gamma_1 & 0 & \gamma_2 & -\mu \end{pmatrix}$$

$$J = \begin{pmatrix} -\beta_1 I_1^* - \phi - \mu & \tau & -\beta_1 S_v^* & 0 & 0 & 0 \\ \phi & -\beta_2 I_1^* - \tau - \mu & -\beta_2 S^* & 0 & 0 & 0 \\ \beta_1 I_1^* & \beta_2 I_1^* & 0 & 0 & 0 & 0 \\ 0 & 0 & \alpha_1 & -(\alpha_2 + \delta_1 + \mu) & 0 & 0 \\ 0 & 0 & 0 & \alpha_2 & -(\delta_2 + \gamma_2 + \mu) & 0 \\ 0 & 0 & \gamma_1 & 0 & \gamma_2 & -\mu \end{pmatrix}$$

We introduce the following shorthand notations to simplify the matrix:

$$\begin{aligned} k_1 &= \beta_1 I_1^* + \phi + \mu, \\ k_2 &= \beta_2 I_1^* + \tau + \mu, \\ k_3 &= \alpha_2 + \delta_1 + \mu, \\ k_4 &= \delta_2 + \gamma_2 + \mu, \\ k_5 &= \mu. \end{aligned}$$

Using these, the Jacobian matrix becomes:

$$J = \begin{pmatrix} -k_1 & \tau & -\beta_1 S_v^* & 0 & 0 & 0 \\ \phi & -k_2 & -\beta_2 S^* & 0 & 0 & 0 \\ \beta_1 I_1^* & \beta_2 I_1^* & 0 & 0 & 0 & 0 \\ 0 & 0 & \alpha_1 & -k_3 & 0 & 0 \\ 0 & 0 & 0 & \alpha_2 & -k_4 & 0 \\ 0 & 0 & \gamma_1 & 0 & \gamma_2 & -k_5 \end{pmatrix}$$

We analyze the stability of the EE based on the trace and determinant of J.

$$\mathrm{Tr}(J) = -(k_1 + k_2 + k_3 + k_4 + k_5) < 0,$$

is clearly negative, indicating that the sum of the eigenvalues is negative. Additionally, the determinant of J:

$$\det(J) = k_3k_4k_5\left(I_1S\beta_1\beta_2\tau + I_1S\beta_2k_1 + I_1S_v\beta_1k_2 + I_1S_v\beta_1\beta_2\phi\right) > 0,$$

is positive, indicating that the product of the eigenvalues is positive.

From the given conditions, it follows that the eigenvalues of J possess negative real parts. This deduction follows from the fact that both the trace and determinant of J indicate that either all eigenvalues are negative, or the system contains a conjugate combination of complex eigenvalues possessing negative real parts [56]. Considering the high sensitivity of the determinant to parameters such as $\tau, \phi, \beta_1, \beta_2, S, S_v$, and I_1, it is crucial to note that stability may depend on these parameters remaining within biologically feasible ranges. To guarantee the stability of EE, it is crucial to keep the parameters such that $\det(J) > 0$ and satisfy the condition $\mathcal{R}_0 > 1$. If these conditions are not met, the EE could become unstable. However, under the current parameter assumptions, the signs of $\mathrm{Tr}(J)$ and $\det(J)$ indicate that the system remains stable at EE E^* . □

2.6.3. Global Stability DFE. By applying the approach outlined by [57], we leverage it to establish the stability of DFE within the context of the EVD.

We rewrite the system in terms of uninfected and infected compartments:

$$X = (S_v, S, R) \quad \text{and} \quad Z = (I_1, I_2, Q)$$

As a result, the system is:

$$\frac{dX}{dt} = F(X, Z), \quad \text{and} \quad \frac{dZ}{dt} = G(X, Z),$$

$$\frac{dZ}{dt} = G(X, Z),$$

Uninfected System:

$$\frac{dS_v}{dt} = p\Lambda + \tau S - \beta_1 S_v I_1 - \phi S_v - \mu S_v$$

$$\frac{dS}{dt} = (1-p)\Lambda + \phi S_v - \tau S - \beta_2 S I_1 - \mu S$$

$$\frac{dR}{dt} = \gamma_2 Q + \gamma_1 I_1 - \mu R$$

Thus,

$$F(X, Z) = (p\Lambda + \tau S - \beta_1 S_v I_1 - \phi S_v - \mu S_v, (1-p)\Lambda + \phi S_v - \tau S - \beta_2 S I_1 - \mu S, \gamma_2 Q + \gamma_1 I_1 - \mu R)$$

Infected System:

$$\frac{dI_1}{dt} = (\beta_1 S_v + \beta_2 S)I_1 - (\alpha_1 + \gamma_1 + \mu)I_1$$

$$\frac{dI_2}{dt} = \alpha_1 I_1 - (\alpha_2 + \delta_1 + \mu)I_2$$

$$\frac{dQ}{dt} = \alpha_2 I_2 - (\delta_2 + \gamma_2 + \mu)Q$$

Thus,

$$G(X, Z) = ((\beta_1 S_v + \beta_2 S)I_1 - (\alpha_1 + \gamma_1 + \mu)I_1, \alpha_1 I_1 - (\alpha_2 + \delta_1 + \mu)I_2, \alpha_2 I_2 - (\delta_2 + \gamma_2 + \mu)Q)$$

At the DFE, the infected compartments $I_1 = I_2 = Q = 0$, and the uninfected compartments are given by:

$$S_v = \frac{\Lambda(\mu p + \tau)}{\mu(\mu + \phi + \tau)}, \quad S = \frac{\Lambda(\mu - \mu p + \phi)}{\mu(\mu + \phi + \tau)}, \quad R^* = 0$$

Thus, the DFE is:

$$X^* = \left(\frac{\Lambda(\mu p + \tau)}{\mu(\mu + \phi + \tau)}, \frac{\Lambda(\mu - \mu p + \phi)}{\mu(\mu + \phi + \tau)}, 0 \right), \quad Z = 0$$

Condition (H1) — Global Stability of the Uninfected Subsystem [58]

The uninfected subsystem $\frac{dX}{dt} = F(X, 0)$ at the DFE has negative eigenvalues because it is linear in S_v, S, R and the terms such as $-(\mu + \phi)$ are negative. Hence, X^* is globally asymptotically stable for the uninfected system, satisfying condition (H1).

Condition (H2) — Metzler Matrix and Non-Negative Terms [57]

The Jacobian matrix of the infected subsystem is:

$$A = \frac{\partial G(X, Z)}{\partial Z}\bigg|_{(X^*, Z=0)} = \begin{pmatrix} -(\alpha_1 + \gamma_1 + \mu + \beta_1 + \beta_2) & 0 & 0 \\ \alpha_1 & -(\alpha_2 + \delta_1 + \mu) & 0 \\ 0 & \alpha_2 & -(\delta_2 + \gamma_2 + \mu) \end{pmatrix}$$

This matrix is classified as Metzler since all of its off-diagonal elements are non-negative.

Additionally,

$$\widehat{G}(X, Z) = \begin{pmatrix} -\beta_1 I_1(1 + S_v) - \beta_2 I_1(1 + S) \\ 0 \\ 0 \end{pmatrix}$$

Since $S_v, S \geq 0$, $\widehat{G}(X, Z) \leq 0$. Thus, condition (H2) is not satisfied.

2.6.4. Global Stability of EE. Adopting the geometric method introduced by [55], the global stability within the Ebola virus model can be studied. This approach provides a framework for proving the global stability under specific conditions: H1-H4 [50].

Theorem 2.3 *For $\mathcal{R}_0 > 1$, the system evolves toward a unique endemic equilibrium, which is both globally attracting and asymptotically stable.*

Proof: Consider the disease dynamics of the Ebola model. The Jacobian matrix corresponding to the above system of equations can be expressed as:

$$J = \begin{bmatrix} \beta_1 S_v + \beta_2 S - (\alpha_1 + \gamma_1 + \mu) & 0 & 0 \\ \alpha_1 & -(\alpha_2 + \delta_1 + \mu) & 0 \\ 0 & \alpha_2 & -(\delta_2 + \gamma_2 + \mu) \end{bmatrix} \tag{2.22}$$

This Jacobian matrix can be written as:

$$J = \Phi - \mu I_{4x4}$$

$$\Phi = \begin{bmatrix} \beta_1 S_v + \beta_2 S - (\alpha_1 + \gamma_1) & 0 & 0 \\ \alpha_1 & -(\alpha_2 + \delta_1) & 0 \\ 0 & \alpha_2 & -(\delta_2 + \gamma_2) \end{bmatrix}$$

We calculate the second additive compound matrix of the Jacobian, which is defined as:

$$J^{[2]} = \Phi^{[2]} - 2\mu I_{4x4} \tag{2.23}$$

where

$$\Phi^{[2]} = \begin{bmatrix} \beta_1 S_v + \beta_2 S - (\alpha_1 + \gamma_1 + \alpha_2 + \delta_1) & 0 & 0 \\ \alpha_2 & \beta_1 S_v + \beta_2 S - (\alpha_1 + \gamma_1 + \delta_2 + \gamma_2) & 0 \\ 0 & \alpha_1 & -(\delta_2 + \gamma_2 + \alpha_2 + \delta_1) \end{bmatrix}$$

With

$$\Phi^{[3]} = (\Phi_1^{[3]}, \Phi_2^{[3]}, \Phi_1^{[3]})^T, \tag{2.24}$$

Using the method expressed by [**?**], we compute:

$$\Phi^{[3]} = \begin{bmatrix} -\phi_{11}^{[3]} & 0 & 0 & 0 \\ \tau & -\phi_{22}^{[3]} & (1-r)\beta S & -r\beta S \\ 0 & \alpha_2 & -\phi_{33}^{[3]} & 0 \\ 0 & -\alpha_1 & 0 & -\phi_{44}^{[3]} \end{bmatrix}$$

Therefore,

$$\begin{aligned} \Phi_1^{[3]} &= (\beta_1 S_v + \beta_2 S - (\alpha_1 + \gamma_1 + \alpha_2 + \delta_1), 0, 0)^T \\ \Phi_2^{[3]} &= (\alpha_2, \beta_1 S_v + \beta_2 S - (\alpha_1 + \gamma_1 + \delta_2 + \gamma_2), 0)^T \\ \Phi_4^{[3]} &= (0, -\alpha_1, (\delta_2 + \gamma_2 + \alpha_2 + \delta_1)^T \end{aligned} \tag{2.25}$$

Now, let $P(x) = \text{diag}(Q, I_2, I_1)$, where I_{4x4} is the identity matrix.
Now,

$$B(t) = P_f P^{-1} + P J^{[2]} P^{-1} + \mu I_{4x4} \tag{2.26}$$

$$B(t) = \text{diag}\left(\frac{Q'}{Q}, \frac{I_2'}{I_2}, \frac{I_1'}{I_1},\right) + P\Phi^{[2]}P^{-1} - \mu I_{4x4}$$

We have that

$$P\Phi^{[3]}P^{-1} = \begin{bmatrix} \beta_1 S_v + \beta_2 S - (\alpha_1 + \gamma_1 + \alpha_2 + \delta_1) & 0 & 0 \\ \alpha_2 q I_2 & \beta_1 S_v + \beta_2 S - (\alpha_1 + \gamma_1 + \delta_2 + \gamma_2) & 0 \\ 0 & \frac{\alpha_1 I_1}{q I_2} & -(\delta_2 + \gamma_2 + \alpha_2 + \delta_1) \end{bmatrix}$$

From the model equation subsystem, we have that

$$\frac{dI_1}{dt} = \beta_1 S_v + \beta_2 S I_1 - (\alpha_1 + \gamma_1 + \mu) I_1$$

This implies that

$$\frac{I_1'}{I_1} = \beta_1 S_v + \beta_2 S - (\alpha_1 + \gamma_1 + \mu)$$

Also, we have that

$$\frac{dI_2}{dt} = \alpha_1 I_1 - (\alpha_2 + \delta_1 + \mu) I_2$$

$$\frac{I_2'}{I_2} = \frac{\alpha_1 I_1}{I_2} - (\alpha_2 + \delta_1 + \mu)$$

This implies that

$$\frac{\alpha_1 I_1}{I_2} = \frac{I_2'}{I_2} + (\alpha_2 + \delta_1 + \mu)$$

Then,

$$\frac{dQ}{dt} = \alpha_2 I_2 - (\delta_2 + \gamma_2 + \mu)Q$$

$$\frac{Q'}{Q} = \frac{\alpha_2 I_2}{Q} - (\delta_2 + \gamma_2 + \mu)$$

This implies that

$$\frac{\alpha_2 I_2}{Q} = \frac{Q'}{Q} + (\delta_2 + \gamma_2 + \mu)$$

Lastly,

$$\frac{dR}{dt} = \gamma_2 Q + \gamma_1 I_2 - \mu R$$

$$\frac{R'}{R} = \frac{\gamma_2 Q + \gamma_1 I_2}{R} - \mu$$

This implies that

$$\frac{\gamma_2 Q + \gamma_1 I_2}{R} = \frac{R'}{R} + \mu$$

By using the above derivations, we have that

$$h_1(t) = b_{11}(t) + \sum_{j \neq 1} |b_{1j}(t)| \tag{2.27}$$

$$h_1(t) = \beta_1 S_v + \beta_2 S - (\alpha_1 + \gamma_1 + \alpha_2 + \delta_1) - \mu + \frac{Q'}{Q} \tag{2.28}$$

$$\leq -(\alpha_2 + \gamma_1) + \frac{I_1'}{I_1} + \frac{Q'}{Q} = \bar{h}_1(t) \tag{2.29}$$

$$h_2(t) = b_{22}(t) + \sum_{j \neq 2} |b_{2j}(t)| \tag{2.30}$$

$$h_2(t) = \beta_1 S_v + \beta_2 S - (\alpha_1 + \gamma_1 + \delta_2 + \gamma_2) - \mu + \frac{I_2'}{I_2} + \frac{\alpha_2 q I_1}{I_2} \tag{2.31}$$

$$\leq -(\delta_2 + \gamma_2) + \frac{I_2'}{I_2} + \frac{\alpha_2 q I_1}{I_2} = \bar{h}_2(t) \tag{2.32}$$

$$h_3(t) = b_{33}(t) + \sum_{j\neq 3} |b_{3j}(t)| \tag{2.33}$$

$$h_3(t) = -(\delta_2 + \gamma_2 + \alpha_2 + \delta_1) - \mu + \frac{\alpha_2 I_2}{Q} \tag{2.34}$$

$$\leq -(\delta_2 + \gamma_2 + \mu) + \bar{h}_3(t) \tag{2.35}$$

We have the option to select W in H4 as:

$$W(t) = \text{diag}(\bar{h}_1(t), \bar{h}_2(t), \bar{h}_3(t), \bar{h}_4(t)) \tag{2.36}$$

Thus

$$\lim_{t\to+\infty} \frac{1}{t} \int_0^t \bar{h}_i(t)dt = \bar{h}_i < 0,$$

Where

$$\begin{aligned}
\bar{h}_1 &= -(\alpha_1 + \gamma_1 + 3\mu) \\
\bar{h}_2 &= -(\alpha_2 + \delta_1 + \mu) \\
\bar{h}_3 &= -(\delta_2 + \gamma_2 + \mu)
\end{aligned}$$

Given that $\mathcal{R}_0 > 1$, the model possesses a unique EE x^*. According to condition (H3), x^* is the only equilibrium within $D \subset \Omega$. The compact absorbing set K (condition (H2)) guarantees that trajectories are bounded. Constructing the matrix $P(x)$ and validating the inequalities involving $b_{ij}(t)$ and $w_{ij}(t)$ (condition (H4)) demonstrate that the directional derivatives comply with the Bendixson criterion. This criterion eliminates the possibility of non-constant periodic solutions, thereby confirming that x^* is asymptotically stable globally [59]. Thus, EE is asymptotically stable globally when $\mathcal{R}_0 > 1$ □

3. Sensitivity Analysis

Sensitivity analysis serves as an essential method for investigating how variations in model parameters influence its behavior. It allows us to determine how variations in each parameter influence the basic reproduction number ($\mathcal{R}_0$). A positive index shows a direct influence on $\mathcal{R}_0$. Specifically, this means that increasing the value of this parameter results in an increase in $\mathcal{R}_0$, reflecting a positive relationship between them. Conversely, a sensitivity index of negative value reflects an inverse relationship, implying that increasing the parameter will lead to a decrease in $\mathcal{R}_0$. This analysis helps identify the most influential parameters, guiding targeted resource allocation for controlling the transmission of the EVD [16]. For this purpose, we utilize the parameter values provided in Table 1 and apply the normalized forward sensitivity index, defined as follows:

$$S_x^{\mathcal{R}_0} = \frac{\partial \mathcal{R}_0}{\partial x} \cdot \frac{x}{\mathcal{R}_0}.$$

$\mathcal{R}_0$ is given as:

$$\mathcal{R}_0 = \frac{\Lambda\left[(\mu - \mu p + \phi)\beta_2 + (\mu p + \tau)\beta_1\right]}{\mu(\mu + \phi + \tau)(\alpha_1 + \gamma_1 + \mu)}$$

1. Sensitivity with respect to Λ:

$$S_\Lambda^{\mathcal{R}_0} = \frac{\partial \mathcal{R}_0}{\partial \Lambda} \cdot \frac{\Lambda}{\mathcal{R}_0}.$$

$$\frac{\partial \mathcal{R}_0}{\partial \Lambda} = \frac{\beta_1(\mu p + \tau) + \beta_2(-\mu p + \mu + \phi)}{\mu(\alpha_1 + \gamma_1 + \mu)(\mu + \phi + \tau)}$$

$$S_{\Lambda}^{\mathcal{R}_0} = \frac{\partial \mathcal{R}_0}{\partial \Lambda} \cdot \frac{\Lambda}{\mathcal{R}_0} = 1.$$

2. Sensitivity with respect to μ:

$$S_{\mu}^{\mathcal{R}_0} = \frac{\partial \mathcal{R}_0}{\partial \mu} \cdot \frac{\mu}{\mathcal{R}_0}.$$

$$\begin{aligned}\frac{\partial \mathcal{R}_0}{\partial \mu} =& \frac{\Lambda(\beta_1 p + \beta_2(1-p))}{\mu(\alpha_1+\gamma_1+\mu)(\mu+\phi+\tau)} - \frac{\Lambda(\beta_1(\mu p+\tau)+\beta_2(-\mu p+\mu+\phi))}{\mu(\alpha_1+\gamma_1+\mu)(\mu+\phi+\tau)^2} \\ &- \frac{\Lambda(\beta_1(\mu p+\tau)+\beta_2(-\mu p+\mu+\phi))}{\mu(\alpha_1+\gamma_1+\mu)^2(\mu+\phi+\tau)} - \frac{\Lambda(\beta_1(\mu p+\tau)+\beta_2(-\mu p+\mu+\phi))}{\mu^2(\alpha_1+\gamma_1+\mu)(\mu+\phi+\tau)}.\end{aligned}$$

Therefore,

$$S_{\mu}^{\mathcal{R}_0} = \left[\frac{\mu(\beta_1 p + \beta_2(1-p))}{(\mu-\mu p+\phi)\beta_2 + (\mu p+\tau)\beta_1} - \frac{\mu}{(\mu+\phi+\tau)} - \frac{\mu}{(\alpha_1+\gamma_1+\mu)} - 1\right].$$

3. Sensitivity with respect to p:

$$S_{p}^{\mathcal{R}_0} = \frac{\partial \mathcal{R}_0}{\partial p} \cdot \frac{p}{\mathcal{R}_0}.$$

$$\frac{\partial \mathcal{R}_0}{\partial p} = \frac{\Lambda(\beta_1\mu - \beta_2\mu)}{\mu(\alpha_1+\gamma_1+\mu)(\mu+\phi+\tau)}$$

$$S_{p}^{\mathcal{R}_0} = \frac{p(-\mu\beta_2 + \mu\beta_1)}{(\mu-\mu p+\phi)\beta_2 + (\mu p+\tau)\beta_1}.$$

4. Sensitivity with respect to ϕ:

$$S_{\phi}^{\mathcal{R}_0} = \frac{\partial \mathcal{R}_0}{\partial \phi} \cdot \frac{\phi}{\mathcal{R}_0}.$$

$$\frac{\partial \mathcal{R}_0}{\partial \phi} = \frac{\Lambda\beta_2}{\mu(\alpha_1+\gamma_1+\mu)(\mu+\phi+\tau)} - \frac{\Lambda(\beta_1(\mu p+\tau)+\beta_2(-\mu p+\mu+\phi))}{\mu(\alpha_1+\gamma_1+\mu)(\mu+\phi+\tau)^2}$$

$$S_{\phi}^{\mathcal{R}_0} = \frac{\phi}{(\mu-\mu p+\phi)\beta_2 + (\mu p+\tau)\beta_1}\left[\beta_2 - \frac{(\beta_1(\mu p+\tau)+\beta_2(-\mu p+\mu+\phi))}{(\mu+\phi+\tau)}\right].$$

Therefore,

$$S_{\phi}^{\mathcal{R}_0} = \frac{\phi\beta_2}{(\mu-\mu p+\phi)\beta_2 + (\mu p+\tau)\beta_1} - \frac{\phi}{(\mu+\phi+\tau)}.$$

5. Sensitivity with respect to β_1:

$$S_{\beta_1}^{\mathcal{R}_0} = \frac{\partial \mathcal{R}_0}{\partial \beta_1} \cdot \frac{\beta_1}{\mathcal{R}_0}.$$

$$\frac{\partial \mathcal{R}_0}{\partial \beta_1} = \frac{\Lambda(\mu p+\tau)}{\mu(\alpha_1+\gamma_1+\mu)(\mu+\phi+\tau)}$$

Therefore,

$$S_{\beta_1}^{\mathcal{R}_0} = \frac{\beta_1(\mu p+\tau)}{(\mu-\mu p+\phi)\beta_2 + (\mu p+\tau)\beta_1}.$$

6. Sensitivity with respect to β_2:

$$S_{\beta_2}^{\mathcal{R}_0} = \frac{\partial \mathcal{R}_0}{\partial \beta_2} \cdot \frac{\beta_2}{\mathcal{R}_0}.$$

$$\frac{\partial \mathcal{R}_0}{\partial \beta_2} = \frac{\Lambda(-\mu p+\mu+\phi)}{\mu(\alpha_1+\gamma_1+\mu)(\mu+\phi+\tau)}$$

Therefore,

$$S_{\beta_2}^{\mathcal{R}_0} = \frac{\beta_2(\mu - \mu p + \phi)}{(\mu - \mu p + \phi)\beta_2 + (\mu p + \tau)\beta_1}.$$

7. Sensitivity with respect to τ:

$$S_{\tau}^{\mathcal{R}_0} = \frac{\partial \mathcal{R}_0}{\partial \tau} \cdot \frac{\tau}{\mathcal{R}_0}.$$

$$\frac{\partial \mathcal{R}_0}{\partial \tau} = \frac{\Lambda\beta_1}{\mu(\alpha_1 + \gamma_1 + \mu)(\mu + \phi + \tau)} - \frac{\Lambda(\beta_1(\mu p + \tau) + \beta_2(-\mu p + \mu + \phi))}{\mu(\alpha_1 + \gamma_1 + \mu)(\mu + \phi + \tau)^2}$$

$$S_{\tau}^{\mathcal{R}_0} = \frac{\Lambda}{\mu(\alpha_1 + \gamma_1 + \mu)(\mu + \phi + \tau)} \left[\beta_1 - \frac{(\beta_1(\mu p + \tau) + \beta_2(-\mu p + \mu + \phi))}{(\mu + \phi + \tau)}\right]$$

Therefore,

$$S_{\tau}^{\mathcal{R}_0} = \frac{\tau\beta_1}{(\mu - \mu p + \phi)\beta_2 + (\mu p + \tau)\beta_1} - \frac{\tau}{(\mu + \phi + \tau)}$$

8. Sensitivity with respect to α_1:

$$S_{\alpha_1}^{\mathcal{R}_0} = \frac{\partial \mathcal{R}_0}{\partial \alpha_1} \cdot \frac{\alpha_1}{\mathcal{R}_0}.$$

$$\frac{\partial \mathcal{R}_0}{\partial \alpha_1} = -\frac{\Lambda(\beta_1(\mu p + \tau) + \beta_2(-\mu p + \mu + \phi))}{\mu(\alpha_1 + \gamma_1 + \mu)^2(\mu + \phi + \tau)}$$

Therefore,

$$S_{\alpha_1}^{\mathcal{R}_0} = -\frac{\alpha_1}{\alpha_1 + \gamma_1 + \mu}.$$

9. Sensitivity with respect to γ_1:

$$S_{\gamma_1}^{\mathcal{R}_0} = \frac{\partial \mathcal{R}_0}{\partial \gamma_1} \cdot \frac{\gamma_1}{\mathcal{R}_0}.$$

$$\frac{\partial \mathcal{R}_0}{\partial \gamma_1} = -\frac{\Lambda(\beta_1(\mu p + \tau) + \beta_2(-\mu p + \mu + \phi))}{\mu(\alpha_1 + \gamma_1 + \mu)^2(\mu + \phi + \tau)}$$

Therefore,

$$S_{\gamma_1}^{\mathcal{R}_0} = -\frac{\gamma_1}{(\alpha_1 + \gamma_1 + \mu)}$$

3.1. Interpretation of Sensitivity Indices

As shown in Table 2, the population recruitment rate (Λ) has a sensitivity index of $S_{\Lambda}^{\mathcal{R}_0} = 1$, indicating a direct proportional relationship with $\mathcal{R}_0$. This highlights that increased population influx significantly drives the epidemic's potential. In contrast, the natural death rate (μ) with $S_{\mu}^{\mathcal{R}_0} = -0.876$ has a strong negative impact, as higher mortality reduces the susceptible and infectious populations, thereby lowering transmission. Similarly, the proportion of vaccinated individuals (p) has a slight negative effect ($S_{p}^{\mathcal{R}_0} = -0.015$), reflecting the minimal role vaccination coverage plays due to the relatively low value of the force of infection among vaccinated individuals (β_1).

Recovery and transmission parameters also show notable effects. The rate at which vaccination wanes (ϕ) has a moderate positive influence ($S_{\phi}^{\mathcal{R}_0} = 0.225$), emphasizing the importance of treatment and post-vaccination immunity. Infection rate for vaccinated individuals (β_1) exerts a minor positive effect ($S_{\beta_1}^{\mathcal{R}_0} = 0.020$), infection rate for susceptible individuals (β_2) is the dominant contributor ($S_{\beta_2}^{\mathcal{R}_0} = 0.955$), highlighting the critical need to control unvaccinated transmission. Other parameters like the quarantine rate (τ) and the transition rate to infectious states (α_1) have negligible ($S_{\tau}^{\mathcal{R}_0} = -0.007$) and significant negative ($S_{\alpha_1}^{\mathcal{R}_0} = -0.725$) impacts, respectively. Finally, increasing recovery rates for infectious individuals (γ_1) moderately reduces $\mathcal{R}_0$ ($S_{\gamma_1}^{\mathcal{R}_0} = -0.274$), showcasing the value of enhancing treatment strategies.

Table 2: Sensitivity Index of the EVD ($\mathcal{R}_0$)

Parameter	**Sensitivity Index** ($S^x_{\mathcal{R}_0}$)
Λ	1.000
μ	-0.876
p	-0.015
ϕ	0.225
β_1	0.020
β_2	0.455
τ	-0.007
α_1	-0.725
γ_1	-0.274

4. Numerical Simulation

Simulations are conducted to explore the impact of vaccination and public enlightenment on the spread of EVD, especially over a long period. In this analysis, the model will be examined using the given parameter values and the estimated initial conditions for the state variables.

The time evolution of each compartment is shown in the following figures, which illustrate how the populations of different categories change over time. The evolution of the latently infected individuals in category 1 are depicted in Figure 3, and those in category 2 are shown in Figure 4. The quarantined population is illustrated in Figure 5, and finally, the recovered population is represented in Figure 6.

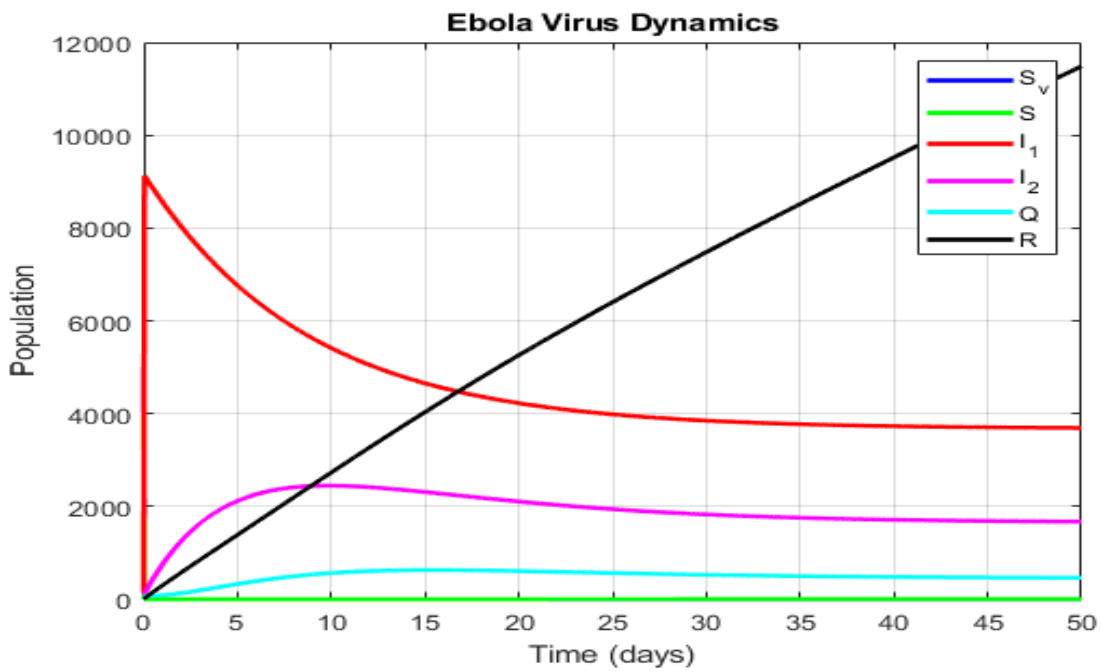

Figure 2: Model flow diagram.

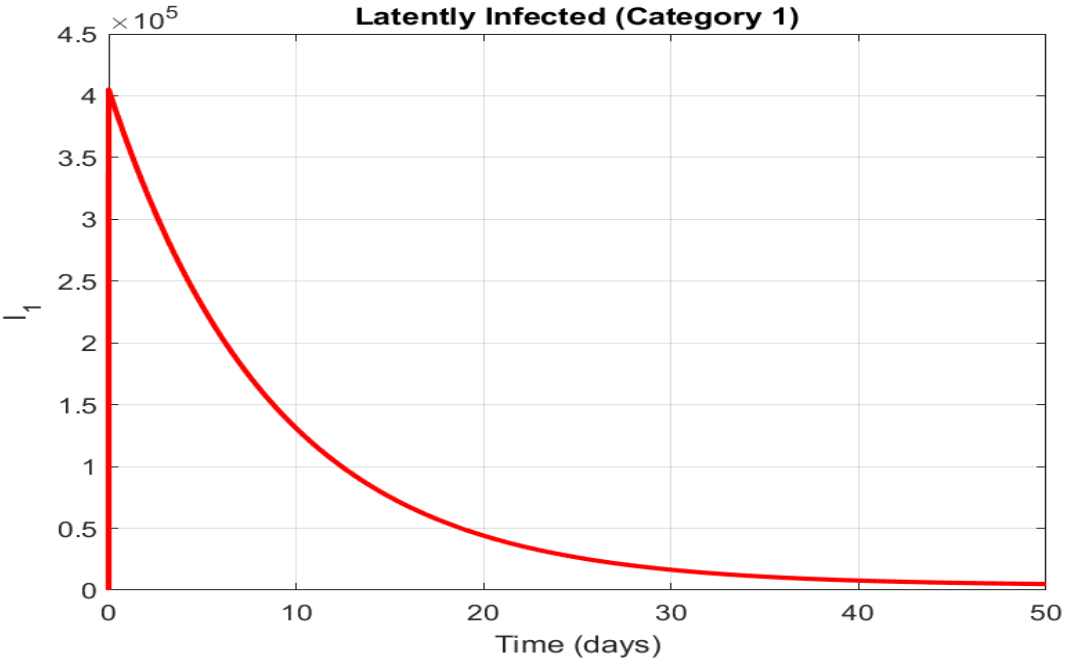

Figure 3: Dynamics of the I_1 population.

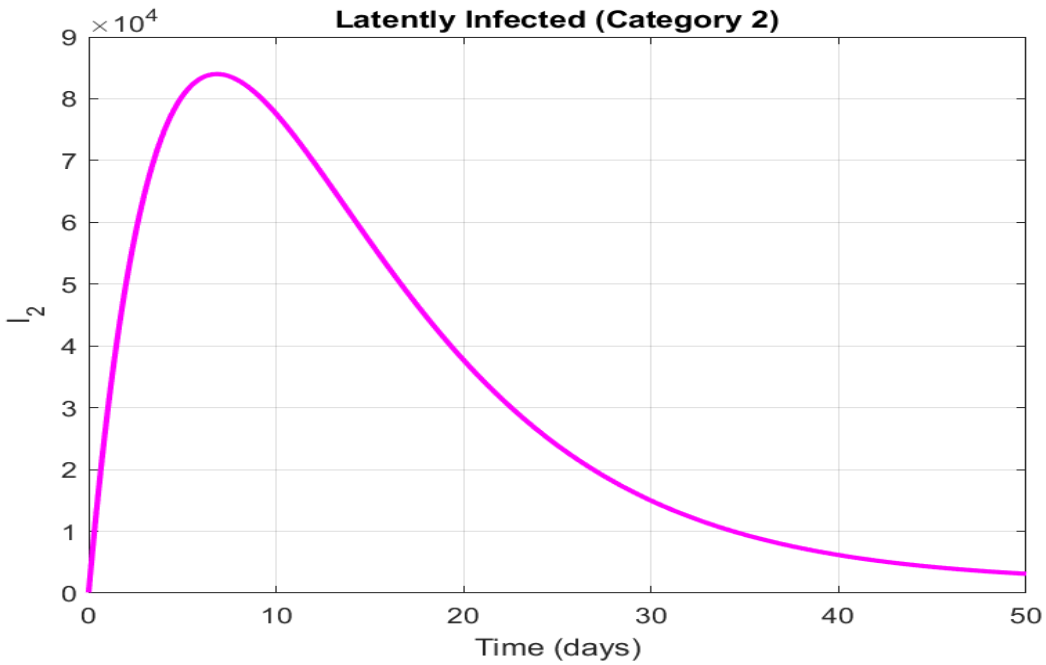

Figure 4: Dynamics of the I_2 population.

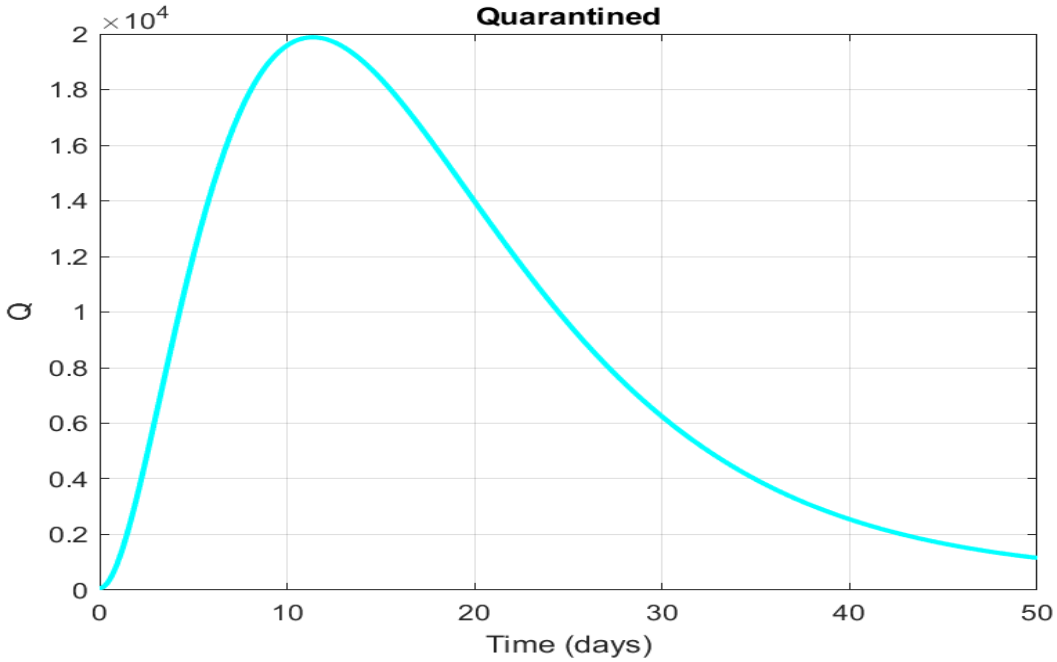

Figure 5: Dynamics of the Q population.

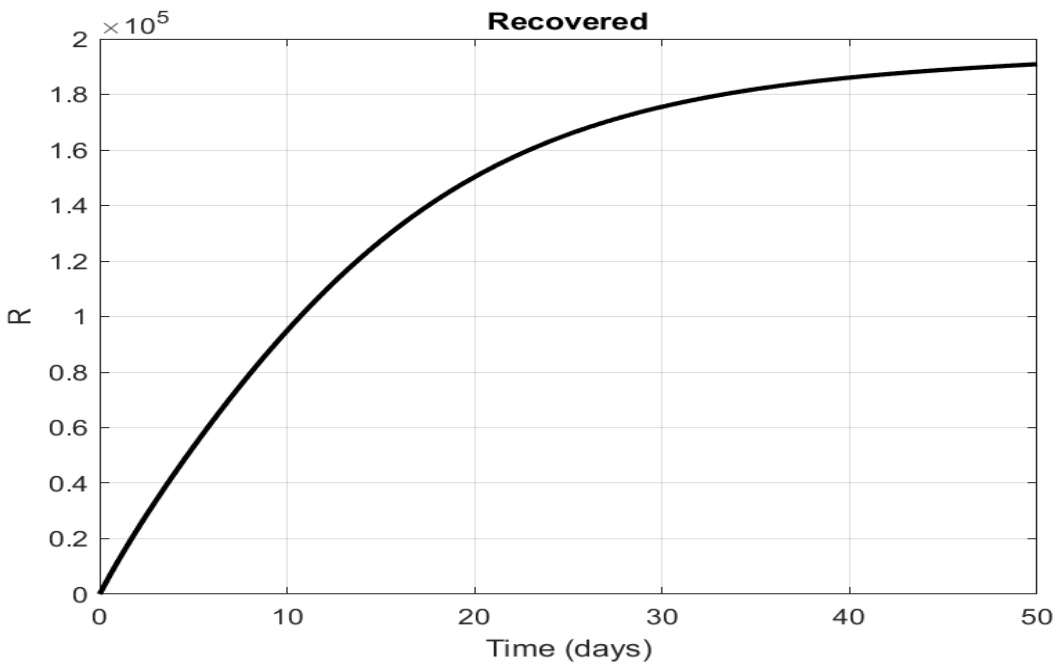

Figure 6: Dynamics of the R population.

4.1. Simulation of the Sensitivity Indices of the EVD

In this section, we present 3D surface plots that visualize the relationship between the $\mathcal{R}_0$, β_2 and τ.

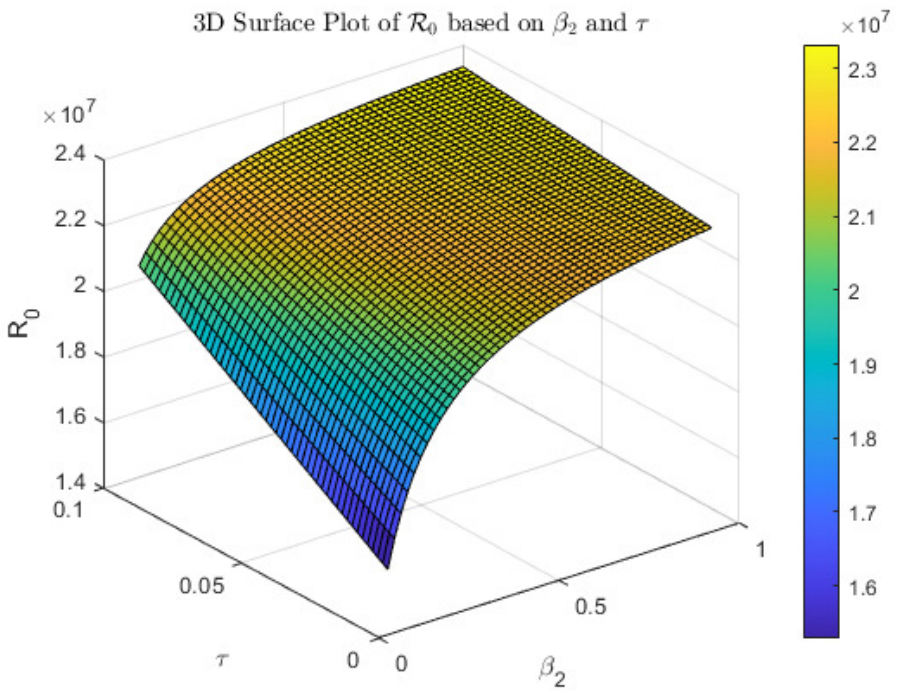

Figure 7: 3D Surface Plot of $\mathcal{R}_0$ based on β_2 and τ

In Figure 7, the infection rate among susceptible individuals (β_2) exerts a strong influence on R_0. High β_2 consistently drives R_0 to higher values, emphasizing the critical need for interventions that directly reduce transmission among this group. The vaccination rate (τ) significantly affects R_0. Low values of τ result in consistently high R_0, emphasizing the critical role of expanding vaccination coverage is essential for effectively controlling the epidemic.. The interaction between β_2 and τ demonstrates that increasing τ is more effective in reducing R_0 when β_2 is low. Conversely, when β_2 is high, even substantial vaccination rates may not suffice, necessitating additional control measures. Policymakers must focus on a combination of strategies, including:

- Reducing transmission through public enlightenment campaigns.
- Increasing vaccination rates.
- Implementing isolation and hygiene measures to minimize contact rates.

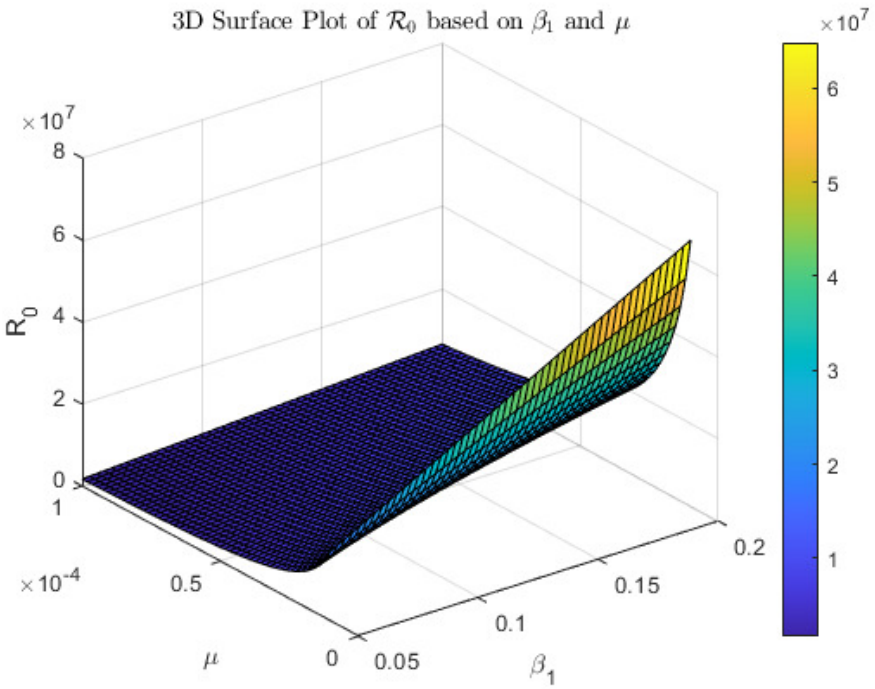

Figure 8: Sensitivity Indices for $\mathcal{R}_0$ based on varying parameters

Figure 8 presents the sensitivity for $\mathcal{R}_0$, μ, and β_1. The infection rate among vaccinated individuals (β_1) has a significant influence on $\mathcal{R}_0$. Higher β_1 values consistently lead to greater transmission potential, highlighting the need for effective vaccination programs that reduce susceptibility to infection among vaccinated individuals. The natural death rate (μ) serves as a moderating factor for $\mathcal{R}_0$. Lower μ values extend the duration of infectiousness in the population, leading to higher $\mathcal{R}_0$. Conversely, higher μ reduces population density and contact rates, mitigating the spread. The combination of high β_1 and low μ creates a synergistic effect that maximizes $\mathcal{R}_0$. This underscores the need for comprehensive interventions that address both vaccination effectiveness and factors influencing population dynamics.

The sensitivity simulations highlight the importance of reducing β_1 through improved vaccination strategies that provide better immunity and minimizing $\mathcal{R}_0$ by addressing demographic factors such as mortality and recruitment rates. Policymakers should:

- Enhance vaccine efficacy to lower transmission among vaccinated individuals.
- Implement non-pharmaceutical interventions to reduce transmission rates.
- Consider population dynamics in the design and implementation of control measures.

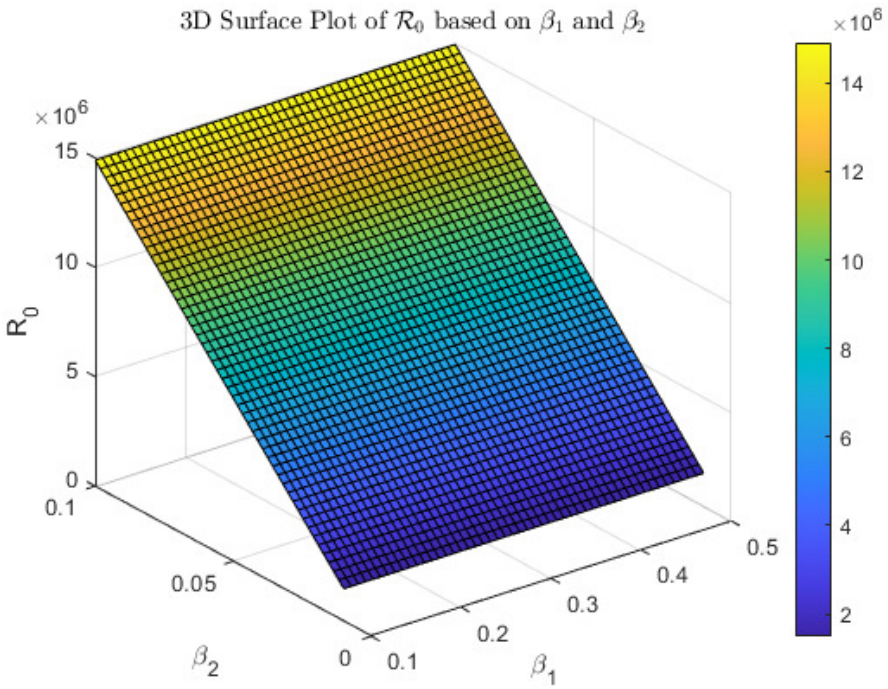

Figure 9: 3D Surface Plot of $\mathcal{R}_0$ based on β_2 and β_2

In Figure 9, the infection rate among susceptible individuals (β_2) has a more pronounced effect on R_0 compared to β_1. High β_2 leads to a disproportionately large R_0, reflecting the critical need to reduce the exposure of susceptible individuals. The infection rate among vaccinated individuals (β_1) significantly impacts R_0 when it is high. This suggests that vaccination alone may not suffice if the vaccine does not adequately reduce susceptibility or if vaccine uptake is low. To control the epidemic, interventions such as increasing vaccination rates (τ), improving vaccine efficacy (lowering β_1), and reducing contact rates (lowering β_2) must work synergistically. The drastic changes in R_0 across different parameter values emphasize the non-linear nature of the epidemic dynamics, necessitating careful parameter monitoring in real-world applications.

5. Conclusion

In this research, we formulated a deterministic model to investigate the transmission of EVD, focusing on the critical control mechanisms of vaccination and public enlightenment. The sensitivity analysis highlights the significant impact of vaccination rates (τ) and the infection rate (β_2) among susceptible individuals on $\mathcal{R}_0$. Our findings demonstrate that the infection rate among susceptible individuals has a dominant effect on $\mathcal{R}_0$, underscoring the need for interventions aimed at reducing transmission within this group. Moreover, vaccination, while essential, must be coupled with high uptake and effectiveness to control the disease spread effectively, particularly in populations at higher risk. Low vaccination rates and high β_2 consistently lead to higher $\mathcal{R}_0$ values, which emphasize the importance of scaling up vaccination coverage. However, when β_2 is high, even substantial increases in vaccination rates may not be sufficient on their own, suggesting the necessity for complementary interventions such as public enlightenment and other control measures.

Our model also reveals a nuanced behavior in its stability analysis. Locally, the model is stable at both DFE and EE. However, while DFE is globally unstable, the EE exhibits global stability. This distinction highlights the importance of reaching and maintaining the EE as a target state, as the DFE may not be sustainable in the long term under realistic conditions.

The study underscores the need for a multifaceted approach to Ebola control. It is critical to focus on reducing transmission among susceptible populations, ensuring high vaccination coverage, and employing complementary strategies such as public enlightenment campaigns and isolation measures. The sensitivity analysis and stability results provide a strong foundation for policymakers to design targeted interventions that can effectively mitigate the spread of Ebola. It is far more effective to prevent Ebola than to manage the disease once it has spread, as supportive care is not 100% effective and recovery from the toxic phase remains uncertain. Hence, vaccination, alongside strategic control measures, remains the most effective approach to tackling the epidemic.

Declarations

The authors hereby declare that they have no affiliations or engagements with any organization or entity that has financial or non-financial interests connected to the topics or materials discussed in this manuscript.

Conflict of Interest

The authors state that they have no conflicts of interest.

References

1. Khan, A. *et al.*, *Estimating the basic reproductive ratio for the Ebola outbreak in Liberia and Sierra Leone*, Infectious Diseases of Poverty **4**, 13 (2015).
2. Taki, E. *et al.*, *Ebanga™: The most recent FDA-approved drug for treating Ebola*, Frontiers in Pharmacology **14**, 1083429 (2023).
3. Feldmann, H., Sprecher, A. and Geisbert, T. W., *Ebola*, New England Journal of Medicine **382**(19), 1832–1842 (2020).
4. Nisar, K. S. *et al.*, *A novel design of evolutionally computing to study the quarantine effects on transmission model of Ebola virus disease*, Results in Physics **48**, 106408 (2023).
5. Abah, R. T. *et al.*, *Mathematical analysis and simulation of Ebola virus disease spread incorporating mitigation measures*, Franklin Open **6**, 100066 (2024).
6. Stein, R. A., *What is Ebola?*, International Journal of Clinical Practice **69**(1), 49–58 (2015).
7. Van Kerkhove, M. *et al.*, *A review of epidemiological parameters from Ebola outbreaks to inform early public health decision-making*, Scientific Data **2**, 150019 (2015).
8. Richardson, E. *et al.*, *Computational mining of B cell receptor repertoires reveals antigen-specific and convergent responses to Ebola vaccination*, Frontiers in Immunology **15**, 1383753 (2024).
9. Wiedemann, A. *et al.*, *Long-term cellular immunity of vaccines for Zaire Ebola Virus Diseases*, Nature Communications **15**, 7666 (2024).
10. Jiang, S. *et al.*, *Mathematical models for devising the optimal Ebola virus disease eradication*, Journal of Translational Medicine **15**, 124 (2017).
11. Dobbs, K. R. *et al.*, *Ebola virus disease in children: epidemiology, pathogenesis, management, and prevention*, Pediatric Research **95**, 488–495 (2024).
12. Sarki, D., Okoye, C., Onah, I. and Mbah, G., *A Nonlinear Model for the Analysis of the Impact of a Comprehensive Treatment and Management of Ebola Virus Disease*, International Journal of Scientific and Engineering Research **9**(5), 1224 (2018).
13. Rafiq, M. *et al.*, *A reliable and competitive mathematical analysis of Ebola epidemic model*, Advances in Difference Equations **2020**, 540 (2020).
14. Nash, R. K. *et al.*, *Ebola virus disease mathematical models and epidemiological parameters: a systematic review*, The Lancet Infectious Diseases (2024).
15. Burk, R. *et al.*, *Neglected filoviruses*, FEMS Microbiology Reviews **40**(4), 494–519 (2016).
16. Ren, H. and Xu, R., *Prevention and control of Ebola virus transmission: mathematical modelling and data fitting*, Journal of Mathematical Biology **89**, 25 (2024).
17. Goldstein, T. *et al.*, *The discovery of Bombali virus adds further support for bats as hosts of ebolaviruses*, Nature Microbiology **3**(10), 1084–1089 (2018).
18. Tomori, O. and Kolawole, M. O., *Ebola virus disease: current vaccine solutions*, Current Opinion in Immunology **71**, 27–33 (2021).
19. Naik, P. A. *et al.*, *Modeling and analysis using piecewise hybrid fractional operator in time scale measure for ebola virus epidemics under Mittag–Leffler kernel*, Scientific Reports **14**, 24963 (2024).

20. Charnley, G. E. C. *et al.*, *Evaluating the risk of conflict on recent Ebola outbreaks in Guinea and the Democratic Republic of the Congo*, BMC Public Health **24**, 860 (2024).

21. Rivers, C. M. *et al.*, *Modeling the impact of interventions on an epidemic of Ebola in Sierra Leone and Liberia*, PLOS Currents Outbreaks **6** (2014).

22. Tadmon, C. and Kengne, J. N., *Enriched spatiotemporal dynamics of a model of Ebola transmission with a composite incidence function and density-independent treatment*, Nonlinear Analysis: Real World Applications **79**, 104118 (2024).

23. Lee, H.-N. *et al.*, *Ebola virus-induced eye sequelae: a murine model for evaluating glycoprotein-targeting therapeutics*, EBioMedicine **104**, 105170 (2024).

24. Yang, W. *et al.*, *Establishment and application of a surrogate model for human Ebola virus disease in BSL-2 laboratory*, Virologica Sinica (2024).

25. Meakin, S. *et al.*, *Effectiveness of rVSV-ZEBOV vaccination during the 2018–20 Ebola virus disease epidemic in the Democratic Republic of the Congo: a retrospective test-negative study*, The Lancet Infectious Diseases (2024).

26. Jacob, S. T. *et al.*, *Ebola virus disease*, Nature Reviews Disease Primers **6**(1), 13 (2020).

27. Geisbert, T. W., *First Ebola virus vaccine to protect human beings?*, The Lancet **389**(10068), 479–480 (2017).

28. Bausch, D. G., *The need for a new strategy for Ebola vaccination*, Nature Medicine **27**, 580–581 (2021).

29. Manno, D. *et al.*, *Safety and immunogenicity of an Ad26.ZEBOV booster dose in children previously vaccinated with the two-dose heterologous Ad26.ZEBOV and MVA-BN-Filo Ebola vaccine regimen: an open-label, non-randomised, phase 2 trial*, The Lancet Infectious Diseases **23**(3), 352–360 (2023).

30. Schwartz, D. A., Anoko, J. N. and Abramowitz, S. A., *Pregnant in the Time of Ebola: Women and Their Children in the 2013-2015 West African Epidemic*, Springer (2019).

31. Schwartz, D. A., *Maternal and infant death and the rVSV-ZEBOV vaccine through three recent Ebola virus epidemics-West Africa, DRC Équateur and DRC Kivu: 4 years of excluding pregnant and lactating women and their infants from immunization*, Current Tropical Medicine Reports **6**, 213–222 (2019).

32. Henao-Restrepo, A. M. *et al.*, *Efficacy and effectiveness of an rVSV-vectored vaccine in preventing Ebola virus disease: final results from the Guinea ring vaccination, open-label, cluster-randomised trial (Ebola Ça Suffit!)*, The Lancet **389**(10068), 505–518 (2017).

33. Larivière, Y. *et al.*, *Ad26.ZEBOV, MVA-BN-Filo Ebola virus disease vaccine regimen plus Ad26.ZEBOV booster at 1 year versus 2 years in health-care and front-line workers in the Democratic Republic of the Congo: secondary and exploratory outcomes of an open-label, randomised, phase 2 trial*, The Lancet Infectious Diseases **24**(7), 746–759 (2024).

34. Choi, E. M.-L. *et al.*, *Safety and immunogenicity of an Ad26.ZEBOV booster vaccine in Human Immunodeficiency Virus positive (HIV+) adults previously vaccinated with the Ad26.ZEBOV, MVA-BN-Filo vaccine regimen against Ebola: A single-arm, open-label Phase II clinical trial in Kenya and Uganda*, Vaccine **41**(50), 7573–7580 (2023).

35. Huttner, A. and Siegrist, C. A., *Durability of single-dose rVSV-ZEBOV vaccine responses: what do we know?*, Expert Review of Vaccines **17**(12), 1105–1110 (2018).

36. Moso, M. A. *et al.*, *Prevention and post-exposure management of occupational exposure to Ebola virus*, The Lancet Infectious Diseases (2023).

37. Pollard, A. J. *et al.*, *Safety and immunogenicity of a two-dose heterologous Ad26.ZEBOV and MVA-BN-Filo Ebola vaccine regimen in adults in Europe (EBOVAC2): a randomised, observer-blind, participant-blind, placebo-controlled, phase 2 trial*, The Lancet Infectious Diseases **21**(4), 493–506 (2021).

38. Afolabi, M. O. *et al.*, *Safety and immunogenicity of the two-dose heterologous Ad26.ZEBOV and MVA-BN-Filo Ebola vaccine regimen in children in Sierra Leone: a randomised, double-blind, controlled trial*, The Lancet Infectious Diseases **22**(1), 110–122 (2022).

39. Ishola, D. *et al.*, *Safety and long-term immunogenicity of the two-dose heterologous Ad26.ZEBOV and MVA-BN-Filo Ebola vaccine regimen in adults in Sierra Leone: a combined open-label, non-randomised stage 1, and a randomised, double-blind, controlled stage 2 trial*, The Lancet Infectious Diseases **22**(1), 97–109 (2022).

40. Choi, E. M. *et al.*, *Immunogenicity of an Extended Dose Interval for the Ad26.ZEBOV, MVA-BN-Filo Ebola Vaccine Regimen in Adults and Children in the Democratic Republic of the Congo*, Vaccines **12**(8), 828 (2024).

41. Kuehn, R. *et al.*, *Vaccines for preventing Ebola virus disease*, Cochrane Database of Systematic Reviews **11**, CD015828 (2024).

42. Thompson, R. *et al.*, *Using real-time modelling to inform the 2017 Ebola outbreak response in DR Congo*, Nature Communications **15**, 5667 (2024).

43. Kwak, M. *et al.*, *A novel indicator in epidemic monitoring through a case study of Ebola in West Africa (2014–2016)*, Scientific Reports **14**(1), 12147 (2024).

44. Xia, Z.-Q. *et al.*, *Modeling the transmission dynamics of Ebola virus disease in Liberia*, Scientific Reports **5**, 13857 (2015).

45. Adu, I. K. *et al.*, *Modelling the dynamics of Ebola disease transmission with optimal control analysis*, Modeling Earth Systems and Environment **10**, 4731–4757 (2024).

46. Shen, M. *et al.*, *Modeling the effect of comprehensive interventions on Ebola virus transmission*, Scientific Reports **5**, 15818 (2015).

47. Kengne, J. N. and Tadmon, C., *Ebola virus disease model with a nonlinear incidence rate and density-dependent treatment*, Infectious Disease Modelling **9**(3), 775–804 (2024).

48. Tahir, M., Anwar, N., Shah, S. I. A. and Khan, T., *Modeling and stability analysis of epidemic expansion disease Ebola virus with implications prevention in population*, Cogent Biology **5**(1), 1619219 (2019).

49. Aguegboh, N. S., Nnaji, D. U., Okongo, W. and Diallo, B., *Modeling the dynamics of onchocerciasis using the atangana-baleanu fractional order with control measures*, Scientific African, e03036 (2025).

50. Diallo, B., Aguegboh, N. S., Osman, S., Dasumani, M. and Okongo, W., *Modelling rabies evolution with vaccination: A fractional calculus perspective*, Scientific African, e03001 (2025).

51. Amanso, O. R., Abonyo, J. O., Kiogora, P. R., Collins, O. and Aguegboh, N., *Analysis of a Mathematical model of Human Papillomavirus transmission dynamics with optimal control for cervical cancer prevention*, Frontiers in Applied Mathematics and Statistics **11**, 1677512 (2026).

52. Nnaemeka, S., Ofe, U., Onyiaji, N. E., Lovelyn, U. O. and others, *Fractional model on the dynamics of chicken pox with vaccination*, International Journal of Mathematics Trends and Technology-IJMTT **67** (2021).

53. Diallo, B., Okelo, J. A., Osman, S., Karanja, S. and Aguegboh, N. S., *A study of fractional bovine tuberculosis model with vaccination on human population*, Communications in Mathematical Biology and Neuroscience **2023**, Article-ID (2023).

54. Aguegboh, N. S., Oranugo, D. O., Kiogora, P. R., Felix, M., Netochukwu, O. and Egwu, A. O., *Existence and uniqueness of solution for a fractional hepatitis b model*, Computational and Mathematical Biophysics **13**(1), 20240009 (2025).

55. Okongo, W., Okelo, J. A., Gathungu, D. K., Moore, S. E. and Nnaemeka, S. A., *Transmission Dynamics of Monkeypox Virus With Age-Structured Human Population: A Mathematical Modeling Approach*, Journal of Applied Mathematics **2024**(1), 9173910 (2024).

56. Aguegboh, N. S., Onyiaji, N., Okeke, C. A., Daniel, N. U., Walter, O. and Diallo, B., *Analysis of a fractional-order prey-predator model with prey refuge and predator harvest using the consumption number: Holling type iii functional response*, Computational and Mathematical Biophysics **13**(1), 20250023 (2025).

57. Aguegboh, N. S., Kiogora, P. R., Felix, M., Okongo, W. and Diallo, B., *Analytic solution of a fractional-order hepatitis model using Laplace Adomian decomposition method and optimal control analysis*, Computational and Mathematical Biophysics **12**(1) (2024).

58. Aguegboh, N. S., Kiogora, P. R., Felix, M. and Diallo, B., *Modeling and control of hepatitis B virus transmission dynamics using fractional order differential equations*, Communications in Mathematical Biology and Neuroscience **2023**, Article-ID (2023).

59. Diallo, B., Dasumani, M., Okelo, J. A., Osman, S., Sow, O., Aguegboh, N. S. and Okongo, W., *Fractional optimal control problem modeling bovine tuberculosis and rabies co-infection*, Results in Control and Optimization **18**, 100523 (2025).

Nnaemeka Stanley Aguegboh,
Department of Mathematical Sciences,
Veritas University Abuja,
Nigeria.
E-mail address: aguegbohn@veritas.edu.ng

and

Chukwudi Okoye,
Department of Mathematics,
University of Nigeria, Nsukka,
Nigeria.
E-mail address: chukwudi.okoye@unn.edu.ng

and

Chinedu Kingsley Friday,
Department of Mathematics,

University of Nigeria, Nsukka,
Nigeria.
E-mail address: chinedu.friday.pg80564@unn.edu.ng

and

Chioma Lydia Ejikeme,
Department of Mathematics,
University of Nigeria, Nsukka,
Nigeria.
E-mail address: chioma.ejikeme@unn.edu.ng